

# SynSeg: Feature Synergy for Multi-Category Contrastive Learning in Open-Vocabulary Semantic Segmentation

Weichen Zhang<sup>1</sup>, Kebin Liu<sup>1,\*</sup>, Fan Dang<sup>3</sup>, Zhui Zhu<sup>2</sup>, Xikai Sun<sup>1</sup>, Yunhao Liu<sup>1,2</sup>

<sup>1</sup>Global Innovation Exchange, <sup>2</sup>Department of Automation, Tsinghua University, Beijing, China

<sup>3</sup>School of Software Engineering, Beijing Jiaotong University, Beijing, China

{weic\_zhang23, z-zhu22, sxk23}@mails.tsinghua.edu.cn, {kebinliu2021, yunhao}@tsinghua.edu.cn, dangfan@bjtu.edu.cn

## Abstract

Semantic segmentation in open-vocabulary scenarios presents significant challenges due to the wide range and granularity of semantic categories. Existing weakly-supervised methods often rely on category-specific supervision and ill-suited feature construction methods for contrastive learning, leading to semantic misalignment and poor performance. In this work, we propose a novel weakly-supervised approach, SynSeg, to address the challenges. SynSeg performs Multi-Category Contrastive Learning (MCCL) as a stronger training signal with a new feature reconstruction framework named Feature Synergy Structure (FSS). Specifically, MCCL strategy robustly combines both intra- and inter-category alignment and separation in order to make the model learn the knowledge of correlations from different categories within the same image. Moreover, FSS reconstructs discriminative features for contrastive learning through prior fusion and semantic-activation-map enhancement, effectively avoiding the foreground bias introduced by the visual encoder. In general, SynSeg effectively improves the abilities in semantic localization and discrimination under weak supervision. Extensive experiments on benchmarks demonstrate that our method outperforms state-of-the-art (SOTA) performance. For instance, SynSeg achieves higher accuracy than SOTA baselines by 4.5% on VOC, 8.9% on Context, 2.6% on Object and 2.0% on City.

## Introduction

Semantic segmentation is a fundamental task in computer vision that focuses on the classification of each pixel in an image with respect to semantic categories. This task has numerous practical applications, including autonomous driving (Cakir et al. 2022; Wang et al. 2022a), medical image analysis (Kar, Nath, and Neog 2021; Jaus et al. 2025) and embodied intelligence (Çağrı Kaymak and Uçar 2018). However, due to the wide range and variability of object categories in the open vocabulary scenarios encountered in real-world tasks, traditional semantic segmentation methods with fixed categories are often insufficient.

To overcome these limitations, many Open Vocabulary Semantic Segmentation (OVSS) approaches have been developed recently (Xu et al. 2022; Mukhoti et al. 2023; Cha,

Mun, and Roh 2023; Lan et al. 2024; Liu et al. 2022; Xing et al. 2023; Wu et al. 2024; Ding, Wang, and Tu 2023). OVSS aims to segment any object category, including those not explicitly defined during training, enabling more flexible and scalable scene understanding. Training such OVSS systems typically requires large amounts of pre-annotated data at pixel level, while semantic annotation in open vocabulary scenarios is both costly and challenging (Cho et al. 2024; Ghiasi et al. 2022; Xu et al. 2023). Manual annotation leads to substantial human labor and is prone to the detrimental effects of poor-quality annotations. In contrast, weakly-supervised learning methods that incorporate semantic text cues into the semantic segmentation tasks via visual-text alignment techniques offer a compelling alternative.

Nevertheless, existing weakly-supervised OVSS solutions often fail to achieve satisfactory performance due to the lack of accurate and concrete supervisory signals. GroupViT (Xu et al. 2022) and ViSeg (Liu et al. 2022) are the earliest approaches in the field of OVSS and have paved the way for numerous subsequent studies (Lai 2024; Luo et al. 2023; Ding, Wang, and Tu 2023; Yi et al. 2023). They introduce a simple image-text alignment architecture, which is shown in Fig. 1(a). Specifically, they operate by grouping local visual features and matching these clusters with text embeddings at test time to generate segmentation masks. However, during training, text embeddings are aligned with a global image representation rather than the detailed region-level features used during inference. This mismatch leads to a notable inconsistency between training and testing, which may impede the model’s ability to fully capture fine-grained semantic details.

Some other approaches like TCL (Cha, Mun, and Roh 2023) improved on the above by introducing region-level visual-text alignment training objective, which is shown in Fig. 1(b). These methods leverage the directional cues provided by textual descriptions to jointly guide the regions’ segmentation in both training and testing process (Wu et al. 2024; Mukhoti et al. 2023). These schemes work well in simple scenes with sparse targets. They, however, encounter a substantial limitation when applied to scenarios with dense targets which are common in real-world open vocabulary settings (Caesar, Uijlings, and Ferrari 2018; Lin et al. 2014). This limitation comes from the fact that each segmentation region usually aligns to just one semantic category. And

\*Corresponding author.

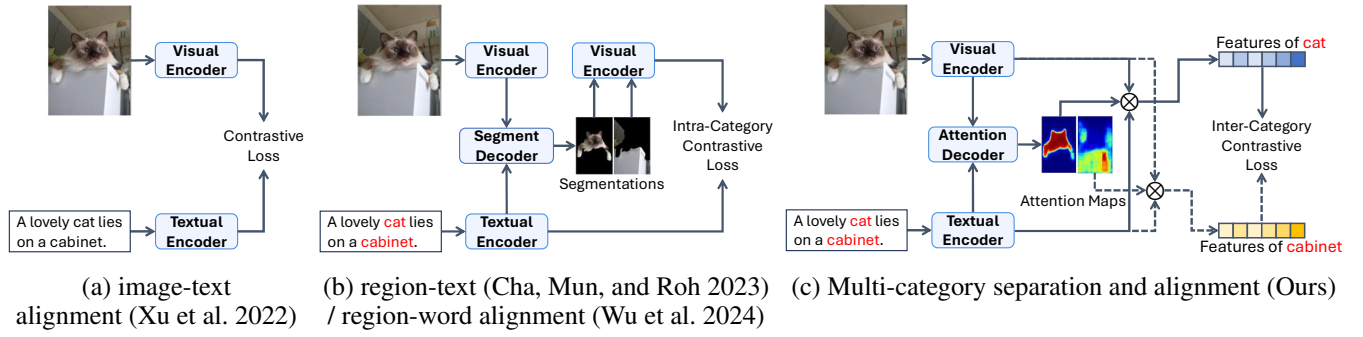


Figure 1: **Training paradigms comparison among previous works and ours.** Prior approaches typically adopt either (a) image-text alignment or (b) region-text/region-word alignment, primarily emphasizing *intra-category* contrastive learning. In contrast, our novel paradigm (c) explicitly incorporates *inter-category* contrastive learning for improved discriminative capability. Also, our approach does not need to reconstruct training features from a pre-trained visual encoder.

the loss functions in these solutions are usually designed in a category-specific way, focusing on only intra-category alignment. After all, in real-world scenes where multiple categories appear in close spatial proximity or even visually overlap with each other, intra-category alignment alone is insufficient to achieve strong semantic discrimination. Without a coordinated interplay of both intra- and inter-category alignment and separation mechanisms, the model struggles to disambiguate between overlapping or visually similar regions. As a result, this leads to the first challenge: *existing OVSS methods lack explicit modeling of inter-category correlations during training, which limits their ability to distinguish semantically different targets in one image.*

Moreover, as shown in Fig. 1(a) and (b), previous works typically rely on frozen, pre-trained vision encoders such as CLIP (Radford et al. 2021) to extract features for contrastive learning *after the decoder*. However, these features often exhibit limited discriminability in background regions, as the encoder is inherently biased toward salient foreground objects (Rao et al. 2022; Ding, Wang, and Tu 2023). Therefore, segmentation regions contaminated by background noise may still yield highly similar representations to clean regions. This hinders the rapid decline of the contrastive loss and reduces the overall learning efficiency. As a result, this leads to the second challenge: *existing methods lack the ability to reconstruct representations that are well-suited for contrastive learning in open-vocabulary semantic segmentation.*

To address the two challenges above, our work introduces an innovative approach, SynSeg, for weakly-supervised open vocabulary semantic segmentation. Specifically, we propose a **Multi-Category Contrastive Learning** strategy, and a new feature reconstruction framework named **Feature Synergy Structure**.

**Multi-Category Contrastive Learning (MCCL)** provides a stronger weakly-supervised signal that introduces inter-category alignment and separation across multiple semantic categories, which is shown in Fig. 1(c). This training strategy constructs positive pairs between foreground features and their corresponding text embeddings, as well as negative pairs from foreground and background features

belonging to the same class. Additionally, it forms positive pairs from background features of these semantic categories, for their backgrounds are often highly overlapped, and negative pairs from different semantic classes within the same image. Our method enhances the distinction between objects in semantic-dense scenarios. This enables the model to better distinguish attention maps corresponding to various objects, resulting in more precise semantic localization and segmentation.

In order to generate features for effective MCCL, we propose a feature reconstruction framework named **Feature Synergy Structure (FSS)**. It generates category-aware features enhanced by attention maps. Unlike TCL’s method of incorporating textual features, we fuse the textual features with image features before generating segmentation proposals, forming a conditional visual vector. This vector encodes the semantic category indicated by the text, and when passed through a transformer decoder, it generates a semantic-activation map. After that, the semantic-activation map is thresholded to generate the final segmentation output.

From another perspective, the semantic-activation map produced by the transformer decoder can be interpreted as a class-specific attention map, representing a continuous-valued response that highlights the semantic relevance of each pixel to a given category. To obtain a synergy feature, we flatten the semantic-activation map and perform a matrix multiplication between it and the conditional visual vector. This step leverages the attention map to refine the conditional visual vector by emphasizing regions with high semantic relevance and suppressing less important regions, thereby producing a more discriminative feature representation. Such a synergy feature is ideal for MCCL: for we can reconstruct a set of synergy features for each semantic category present in the image, facilitating improved representation and more robust contrastive learning across multiple classes. Also, we avoid using visual encoder twice and reduce the foreground bias it introduces.

The solutions we propose effectively address the limitations of current weakly-supervised methods in OVSS and enhance segmentation performance. Our primary contributions include:

(1) We introduce a novel Multi-Category Contrastive Learning (MCCL) strategy that incorporates both inter-category and intra-category contrastive objectives, which provides a stronger weak-supervision signal for OVSS task.

(2) We propose a Feature Synergy Structure (FSS) to reconstruct semantic-aware features for effective contrastive learning instead of reusing pretrained visual encoders. The features are enhanced by attention maps, also referred to as semantic-activation maps, which emphasize semantically relevant regions while suppressing less informative areas.

(3) We implement and evaluate our proposed method, SynSeg, across multiple OVSS evaluation datasets, achieving performance that surpasses state-of-the-art (SOTA) benchmarks.

## Related Work

In this section, we will briefly present related works that serve as a motivation for our study.

### Visual-Language Models

Vision-language models aim to bridge the gap between visual and textual modalities, enabling a broad range of multi-modal tasks such as image-text retrieval (Li et al. 2021; Radford et al. 2021), image captioning (Li et al. 2022; Zhang et al. 2021), open-vocabulary detection and recognition (Tang et al. 2024; Wang et al. 2022b; Kim et al. 2022; Wang et al. 2024b), and multi-source semantic segmentation (Deng et al. 2023; Guo et al. 2024). Among these models, CLIP (Contrastive Language-Image Pretraining) (Radford et al. 2021) introduced a framework for joint visual and textual representation learning using contrastive learning on a large-scale dataset of image-text pairs. It aligns image and text embeddings in a shared feature space, enabling zero-shot tasks and fundamental abilities. BLIP (Bootstrapped Language-Image Pretraining) (Li et al. 2022) enhances vision-language models with a multi-modal encoder-decoder architecture and combined generative and contrastive objectives. Its bootstrapped self-learning improves performance across datasets, making it effective for tasks such as image captioning and vision-language understanding.

### Weakly-Supervised Open-Vocabulary Semantic Segmentation

In early OVSS works (Xu et al. 2022; Liu et al. 2022; Luo et al. 2023), textual information does not participate in the computation or generation of segmentation masks but only plays a role in the subsequent matching of mask proposals with candidate semantic labels. Multiple later works follow this structure and explore improvements in segmentation accuracy and semantic alignment precision (Chen et al. 2023; Cai et al. 2023; Lai 2024; Xing et al. 2023). However, with such structure, the visual segmentation output remains unchanged regardless of the provided textual prompt. Furthermore, in the architectures based on the classic GroupViT (Xu et al. 2022), the number of output class token is fixed (e.g., 4 or 8), making it impossible to segment more semantic categories than this predefined limit.

Since the text is not involved in the generation of mask proposals, and only a limited number of semantically irrelevant proposals are produced, this structure necessitates an additional step for global-level alignment, which in turn limits the overall learning efficiency. The inconsistency between region-level alignment during testing and global-level alignment during training also leads to poor performance in fine-grained segmentations.

TCL (Cha, Mun, and Roh 2023) performs a different structure firstly to partially incorporate text labels into the mask generation process and apply region-text alignment during training. Typically, this occurs at the final step, where each pixel feature is compared with text label embeddings to cluster and assign it to a candidate label, determining which pixels are highly correlated with the semantic information to produce the final segmentation result. This paradigm is followed by later works (Mukhoti et al. 2023; Wang et al. 2024a; Sun et al. 2024). For example, CoDe (Wu et al. 2024) improves its work by introducing region-word alignment. In these works, the integration of textual information with the visual feature enables the mask proposal to refer to certain semantic more flexibly, thereby enhancing the granularity of segmentation alignment. However, This training approach mainly focuses on a single object or semantic category and does not exploit the relationships among different semantic objects within the same image.

Furthermore, these works typically feed segmentation results into the CLIP models (Radford et al. 2021) again to construct visual features for loss computing. Since the CLIP model is inherently biased toward salient foreground objects, its visual representations tend to be sparse and less discriminative in background regions (Rao et al. 2022; Ding, Wang, and Tu 2023). In OVSS, when segmentation predictions inadvertently include background noise—pixels that actually belong to other semantic categories—such sparse representations hinder the model’s ability to produce more accurate and precise segmentation regions. Due to CLIP’s limited capacity for representing background content, the visual features of noisy segmentation regions often remain highly similar to those of cleaner regions, which serve as the intended training targets. This leads to optimization bottlenecks of the loss functions’ decline that weaken the effectiveness of contrastive learning, both in terms of intra- and, if applicable, inter-category alignment and separation.

## Approach

In this section, we present the overall pipeline design along with detailed descriptions of the key components.

### Overview of SynSeg

Our pipeline, named SynSeg, is illustrated in Fig. 2. The pre-trained CLIP (Radford et al. 2021) visual and textual encoders process the input image and text labels, respectively, to extract single-modal embeddings. These embeddings are then fused using a Feature-wise Linear Modulation (FiLM) (Perez et al. 2018) module. Specifically, the FiLM module contains a small learnable MLP that takes the text features as input and outputs channel-wise scaling and

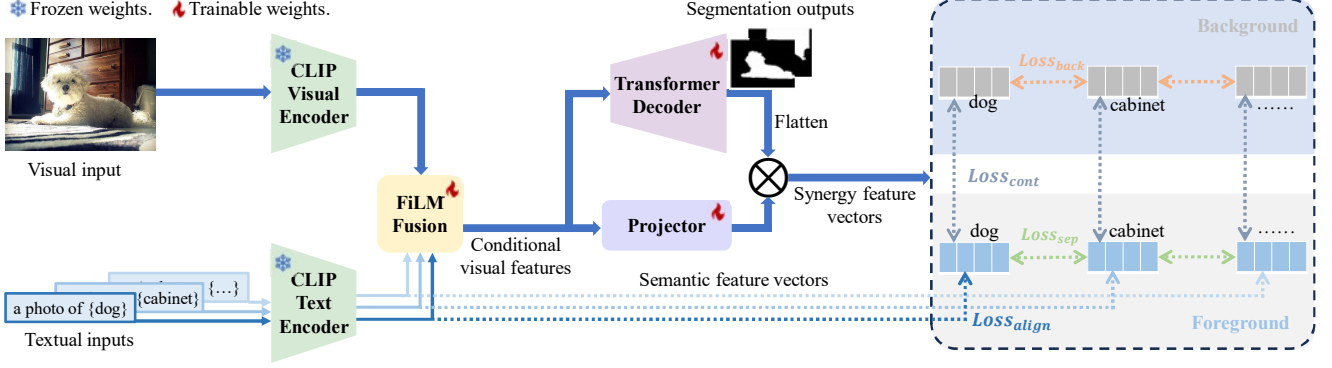


Figure 2: **The pipeline of SynSeg.** It illustrates the proposed Feature Synergy Structure and Multi-Category Contrastive Learning framework. During training, FiLM (Perez et al. 2018) fusion module, transformer decoder and the projector stay trainable, while the CLIP (Radford et al. 2021) encoders stay frozen. The projector is here to make sure the feature vectors in an appropriate dimension for later use.

shifting parameters. These parameters are then directly applied to the visual features to generate the conditional visual vectors. Meanwhile, textual embeddings are stored as semantic feature vectors for intra-category alignment later. During inference, the conditional visual features are passed through the decoder, generating semantic-activation maps, which are similar to class activation mapping (CAM) (Zhou et al. 2016). Then, the semantic-activation maps are thresholded to generate the final segmentation outputs.

### Feature Synergy Structure

In the training phase, we introduce a new feature reconstruction framework, named Feature Synergy Structure (FSS), inspired by CCAM (Xie et al. 2022). Our focus is on the post-decoder reconstruction of features after the segmentation stage, and these reconstructed features are then fed into the subsequent contrastive learning. Rather than running the visual encoder a second time, we rely on FSS to perform this reconstruction.

The semantic-activation maps, which are class-specific heat maps, represent the continuous per-pixel response strength to a given semantic category and can be considered as attention maps for feature enhancement. Instead of applying thresholding, the semantic-activation maps are flattened and subsequently fused with conditional visual features, which are first projected to a compatible dimension via a convolutional-layer-based projector. This fusion is performed through matrix multiplication to generate the synergy feature vectors. By flattening and weighting with semantic activation maps, the synergy vector emphasizes spatial regions with high semantic relevance, preserving contextual cues.

To ensure spatial-semantic consistency, the semantic-activation maps are duplicated and transposed such that each synergy feature vector corresponds to either the foreground or background region of the referred semantic category. Consequently, the synergy features can be separated into category-specific foreground and background representations, respectively. We can generate a set of foreground

and background synergy features corresponding to each semantic category within a single image, which can provide richer and more diverse positive and negative sample pairs for effective MCCL later. This feature fusion mechanism enables the integration of semantic context and fine-grained visual cues, thereby enhancing the discriminative power and expressiveness of the learned representations.

Throughout the training process, only the FiLM fusion module, the projector, and the transformer decoder parameters are updated, while the CLIP visual and textual encoders remain frozen. This ensures the effective leverage of the rich features from the pre-trained visual language model.

### Multi-Category Contrastive Learning

We propose Multi-Category Contrastive Learning (MCCL) as weak supervision training objective tailored for OVSS scenarios. This strategy not only considers the intra-category correlation, but also introduces rich inter-category knowledge. Specifically, it integrates four loss functions as contrastive objectives that collaboratively and adversarially optimize semantic localization. Cosine similarity is used as the distance metric in the high-dimensional space for both positive and negative sample pairs. Note that we clip the cosine similarities into  $[0.005, 0.995]$ , so the values remain positive.

Formally, for a given image  $I$ , let  $\mathcal{C}_I = \{c_1, c_2, \dots, c_{N_I}\}$  denote the set of  $N_I$  semantic categories (or object classes) present in the image, where  $N_I$  varies across different images. Through our model, for each category  $c_i \in \mathcal{C}_I$ , we generate a pair of *synergy feature vectors* that correspond to the visual foreground and background regions guided by the semantic-activation map of  $c_i$ . These feature vectors are denoted as  $f_{c_i}$  and  $\bar{f}_{c_i}$ , respectively. The complete sets of foreground and background synergy features for image  $I$  can thus be expressed as:

$$\mathcal{F}_I = \{f_{c_i} \mid c_i \in \mathcal{C}_I\}, \quad \bar{\mathcal{F}}_I = \{\bar{f}_{c_i} \mid c_i \in \mathcal{C}_I\}. \quad (1)$$

To further integrate textual information, we leverage the CLIP text encoder to generate semantic feature vectors for the text prompts associated with the semantic categories, incorporating them into the Multi-Category Con-

trastive Learning framework:

$$\mathcal{T}_I = \{t_{c_i} = \text{CLIP}_t(c_i) \mid c_i \in \mathcal{C}_I\} \quad (2)$$

where  $\text{CLIP}_t(\cdot)$  denotes the CLIP text encoder, and  $t_{c_i} \in \mathbb{R}^d$  is the  $d$ -dimensional semantic embedding of category  $c_i$ . These semantic feature vectors serve as anchors for intra-category semantic alignment.

To encourage intra-category semantic alignment between the visual synergy features and the corresponding textual representations, we introduce the first loss function,  $L_{\text{align}}$ . For a given image  $I$ , this loss maximizes the cosine similarity between each foreground synergy feature  $f_{c_i} \in \mathcal{F}_I$  and its corresponding semantic feature  $t_{c_i} \in \mathcal{T}_I$ , across all categories  $c_i \in \mathcal{C}_I$ . The alignment loss is defined as:

$$L_{\text{align}}(\mathcal{F}_I, \mathcal{T}_I) = -\frac{1}{N_I} \sum_{c_i \in \mathcal{C}_I} \log(\text{sim}(f_{c_i}, t_{c_i})), \quad (3)$$

where  $\text{sim}(\cdot, \cdot)$  denotes the cosine similarity function, and  $N_I = |\mathcal{C}_I|$  is the number of semantic categories present in image  $I$ .

To enhance the quality of segmentation boundaries, we introduce the second loss function,  $L_{\text{cont}}$ , which performs intra-category separation through contrastive learning between foreground and background regions of the same semantic category. For each category  $c_i \in \mathcal{C}_I$ , this loss minimizes the cosine similarity between the corresponding foreground and background synergy feature vectors  $f_{c_i} \in \mathcal{F}_I$  and  $\bar{f}_{c_i} \in \bar{\mathcal{F}}_I$ . The contrastive loss is defined as:

$$L_{\text{cont}}(\mathcal{F}_I, \bar{\mathcal{F}}_I) = -\frac{1}{N_I} \sum_{c_i \in \mathcal{C}_I} \log(1 - \text{sim}(f_{c_i}, \bar{f}_{c_i})), \quad (4)$$

where  $N_I = |\mathcal{C}_I|$  is the number of categories in image  $I$ .

Inter-category alignment loss is set to limit the unlimited expansion of the foreground segmentation. It also aligns background synergy features corresponding to different categories within the same image, since background regions associated with different categories often exhibit spatial overlap. For a given image  $I$ ,  $L_{\text{back}}$  maximizes the cosine similarity between all background synergy features  $\bar{f}_{c_i} \in \bar{\mathcal{F}}_I$  associated with each category  $c_i \in \mathcal{C}_I$ . It is defined as:

$$L_{\text{back}}(\bar{\mathcal{F}}_I) = -\frac{1}{N_I^{\text{pair}}} \sum_{c_j, c_k \in \mathcal{C}_I} \log(\text{sim}(\bar{f}_{c_j}, \bar{f}_{c_k})) \quad (5)$$

where  $\bar{f}_{c_j}, \bar{f}_{c_k} \in \bar{\mathcal{F}}_I$  are the background synergy features for categories  $c_j$  and  $c_k$ , and  $N_I^{\text{pair}} = N_I^2$  is the number of category pairs in image  $I$ .

To enhance the inter-category separation of individual semantic areas within the same image, we introduce the fourth loss function,  $L_{\text{sep}}$ , as a key component of our Multi-Category Contrastive Learning framework. For a given image  $I$ , this loss minimizes the cosine similarity between foreground synergy features associated with different semantic categories, promoting inter-category feature disentangle-

ment. It is formally defined as:

$$L_{\text{sep}}(\mathcal{F}_I) = -\frac{1}{N_I^{\text{pair}}} \sum_{c_j, c_k \in \mathcal{C}_I} \log(1 - \text{sim}(f_{c_j}, f_{c_k})), \quad (6)$$

where  $f_{c_j}, f_{c_k} \in \mathcal{F}_I$  are the foreground synergy features corresponding to semantic categories  $c_j$  and  $c_k$  in image  $I$ , and  $N_I^{\text{pair}} = N_I^2$  denotes the number of category pairs in  $\mathcal{C}_I$ .

Based on the four loss functions described above, we define the total loss  $L_{\text{total}}$  as a weighted sum of all components, with each term controlled by a corresponding hyperparameter  $\lambda_1, \lambda_2, \lambda_3$ , and  $\lambda_4$ . The total loss is given by:

$$L_{\text{total}} = \lambda_1 L_{\text{align}} + \lambda_2 L_{\text{cont}} + \lambda_3 L_{\text{back}} + \lambda_4 L_{\text{sep}}. \quad (7)$$

The loss functions defined above constitute a weakly-supervised training framework that relies solely on RGB images and their associated category text labels. Our proposed MCCL provides a significantly richer and more informative weak supervision signal compared to existing contrastive learning approaches, which typically operate on intra-category manner only.

## Experiments

In this section, we describe the implementation details of our experiments and report the corresponding results.

### Experiment Setup

**Training datasets.** We use the public conceptual-12m (CC12M) (Changpinyo et al. 2021) as training dataset. After using the NLP functions from the SpaCy library (Honnibal and Montani 2017), nouns and noun phrases are extracted from these captions. Non-referential or irrelevant terms such as direction and unit nouns (e.g., southwest, pair, front) are filtered out, leaving meaningful text labels that provide weak supervision for the associated images. We resize the figures to the same pixel size of  $224 \times 224$  for training.

**Evaluating datasets.** To evaluate the open vocabulary semantic segmentation performance of our method, we test it on five commonly used challenging datasets: PASCAL VOC (VOC) (Everingham et al. 2010), Pascal Context (Context) (Mottaghi et al. 2014), City Scapes (City) (Cordts et al. 2016), COCO Object (Object) and COCO Stuff (Stuff) (Lin et al. 2014; Caesar, Uijlings, and Ferrari 2018). Also, it should be noted that evaluations on VOC and Object treat unlabeled regions as an explicit category *background*, whereas those on Context, Stuff and City focus solely on labeled categories.

**Baselines.** To provide a comprehensive comparison, we select not only the latest but also classical weakly-supervised learning methods as baselines. The eight representative baselines are listed below: GroupViT (Xu et al. 2022), ViewCo (Ren et al. 2023), CoCu (Xing et al. 2023), OVSegmentor, TCL (Cha, Mun, and Roh 2023), CoDe (Wu et al. 2024), MGCA (Liu et al. 2025) and S-Seg (Lai 2024). All baseline methods are assumed to use a pre-trained ViT-B/16 vision backbone for fair comparison, except S-Seg (Lai 2024), which does not specify the type of vision model used in its paper. These methods may use extra training datasets

Method	Publication	Training Datasets	VOC	Context	Object	Stuff	City	Avg.
GroupViT	CVPR 2022	CC3M+CC12M+RedCaps12M	50.4	23.4	27.5	15.3	11.1	25.5
ViewCo	ICLR 2023	CC12M+YFCC14M	52.4	23.0	23.5	–	–	–
CoCu	NeurIPS 2023	CC3M+CC12M+YFCC14M	51.4	–	22.7	15.2	22.1	–
OVSegmentor	CVPR 2023	CC12M	53.8	20.4	25.1	–	–	–
TCL	CVPR 2023	CC3M+CC12M	55.0	33.9	31.6	22.4	24.0	33.4
CoDe	CVPR 2024	CC3M+CC12M	<u>57.7</u>	30.5	<u>32.3</u>	<b>23.9</b>	<u>28.9</u>	34.7
MGCA	TMC 2025	CC3M	53.1	33.7	31.9	22.0	24.0	32.9
S-Seg	CVPR 2025	CC3M+CC12M	53.2	27.2	30.3	–	–	–
SynSeg (Ours)	–	CC12M	<b>62.2</b>	<b>41.8</b>	<b>34.9</b>	<u>23.6</u>	<b>30.9</b>	<b>38.7</b>

Table 1: **Zero-shot semantic segmentation comparisons among weakly-supervised OVSS methods on five representative datasets.** Bold indicates best performance; underlined values are second-best. Results are in mIoU (%), which higher is better.

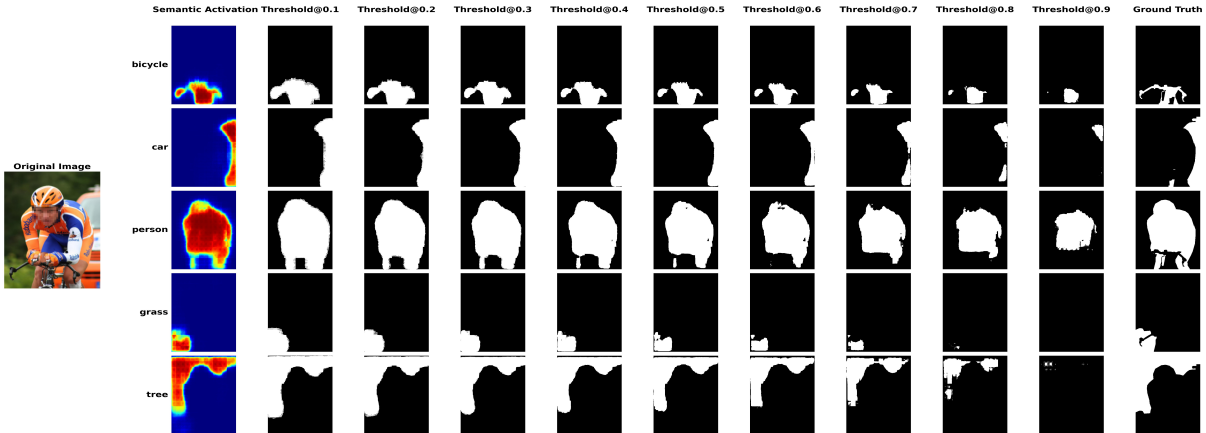


Figure 3: Visual effects of the semantic activation maps and segmentations under different thresholds.

such as CC3M (Sharma et al. 2018), YFCC14M (Thomee et al. 2016) and RedCaps12M (Desai et al. 2021).

**Training Details.** We use a pre-trained CLIP ViT-B/16 model as the encoder. The decoder follows the design of CLIPSeg (Lüddecke and Ecker 2022) and is initialized with the pre-trained weights from CLIPseg. For training, we keep the encoder frozen and only the decoder and the FiLM fusion module remain trainable. All of the experiments are performed on an RTX 4090 GPU.

## Main Results

We compare our proposed method, SynSeg, against a range of classic and latest weakly-supervised open-vocabulary semantic segmentation approaches that rely on text annotations, across five widely-used benchmark datasets (Tab. 1). The table reports the mean Intersection-over-Union (mIoU) score for each method on individual datasets. The **result in boldface** achieves the best performance and the **underlined result** is the second best. SynSeg achieves the best overall performance, with an average mIoU of **38.7%**, outperforming all baselines by a significant margin. Notably, our method sets a new state-of-the-art on four out of five datasets: VOC (**62.2%**), Context (**41.8%**), Object (**34.9%**),

and City (**30.9%**).

## Ablation Study

We examine the effectiveness of the four training objectives by evaluating the impact on segmentation performance of all four loss functions across three representative datasets: Context (Mottaghi et al. 2014), Object (Lin et al. 2014) and Stuff (Caesar, Uijlings, and Ferrari 2018). The results, presented in Tab. 2, show that the combination of all four losses yields the best performance. Removing any single loss leads to a measurable drop in performance, underscoring the complementary contributions of each component in enhancing feature discrimination and segmentation quality. In particular, the inter-category separation loss  $L_{sep}$  is the most prominent because the drop is the largest after it is removed.

## Visual Effects

In this subsection, we present two types of visual examples to demonstrate the segmentation performance of our method, SynSeg, and also in comparison with existing baselines. The examples are selected from the Context dataset (Mottaghi et al. 2014), as it is a common benchmark supported by all baseline methods.



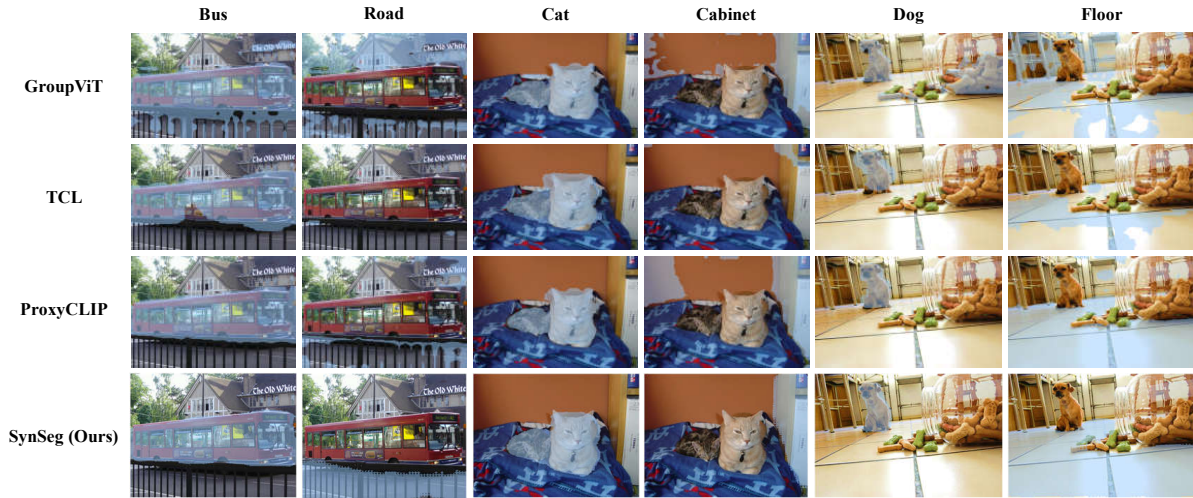


Figure 4: **Segmentation visual comparisons.** The light blue regions indicate the segmentation predictions. The baselines’ results are visually compared with our method, SynSeg.

Loss				MIoU(%)		
$L_{align}$	$L_{cont}$	$L_{back}$	$L_{sep}$	Context	Object	Stuff
Yes	Yes	Yes	Yes	41.8	34.9	23.6
Yes	Yes	Yes	No	39.6	31.0	20.9
Yes	Yes	No	Yes	41.4	34.0	22.9
Yes	No	Yes	Yes	41.5	34.3	23.2
No	Yes	Yes	Yes	41.4	34.2	23.2

Table 2: Ablation study on the training objectives.

We begin by presenting a qualitative example of semantic activation maps and the corresponding segmentation masks predicted by our model under multiple threshold settings, as illustrated in Fig. 3. The example involves five semantic categories: bicycle, car, person, grass, and tree. Unlike traditional OVSS where pixel-level predictions are mutually exclusive (Xu et al. 2022; Cha, Mun, and Roh 2023), our semantic activation maps allow a single pixel to be activated by multiple categories simultaneously. This fits the nature in real-world environments, especially when the objects are physically entangled, for example, between the *head* and the *person*.

Also, we observe that the segmentation results remain visually consistent across a wide range of thresholds, nearly from 0.1 to 0.6, particularly for prominent object categories such as person and taxi. This indicates that the model has an accurate semantic localization ability so that it produces clear boundaries. Moreover, for less salient or texture-heavy classes like grass, where activation may be weaker or more diffused, the model still successfully captures the core regions while gracefully discarding noise at lower thresholds. This demonstrates the model’s ability to balance coarse and fine semantics through a unified representation framework.

In addition, we conduct visual comparisons between our method and existing methods. Our comparison includes weakly-supervised approaches GroupViT (Xu et al. 2022)

and TCL (Cha, Mun, and Roh 2023), and a strong training-free baseline ProxyCLIP (Lan et al. 2024). ProxyCLIP utilizes a large-scale pretrained Vision Foundation Model (VFM) DINO (Jose et al. 2024) for OVSS task. As shown in Fig. 4, our method consistently demonstrates more accurate semantic localization and finer-grained segmentation. The predicted segmentations from our model are better aligned with the object boundaries and exhibit fewer false positives.

In general, our segmentation results show superior performance in both salient and background categories. For salient objects such as bus, cat, and dog, our model produces tighter and more precise boundaries, with reduced over-segmentation compared to others which only ProxyCLIP performs competitively. For background regions such as floor and road, our method significantly outperforms all baselines. ProxyCLIP tends to misclassify visually similar areas as background categories, while GroupViT and TCL often fail to produce coherent masks in these regions. These observations further demonstrate the robustness of our method.

## Conclusion

We propose a novel approach, SynSeg, for open-vocabulary semantic segmentation, integrating Feature Synergy Structure (FSS) with Multi-Category Contrastive Learning (MCCL). Our approach effectively addresses two key challenges in weakly-supervised OVSS: (1) the lack of explicit inter-category correlation injection during training, and (2) the absence of a suitable way of feature reconstruction tailored for contrastive learning. To address these issues, we introduced MCCL that constructs both intra- and inter-category contrastive learning to enhance the weakly-supervised signal. In addition, FSS generates category-aware features by fusing conditional visual embeddings with semantic-activation maps, enabling finer semantic representation for effective MCCL. Experiments on five benchmarks demonstrate the effectiveness of our method. SynSeg con-

---

**Algorithm 1: Noun Phrase Extraction from Captions**

---

**Input:** Caption file with image-caption pairs  
**Output:** Mapping from image to noun phrases

```
1: for each line in the caption file do
2:   Parse caption using spaCy
3:   noun_phrases  $\leftarrow []$ 
4:   for each chunk in parsed.noun_chunks do
5:     Filter tokens with pos_ == NOUN
6:     if at least one noun is retained then
7:       Join tokens and append to noun_phrases
8:     end if
9:   end for
10: end for
11: return image  $\rightarrow$  noun_phrases
```

---

sistently outperforms existing weakly-supervised baselines, achieving state-of-the-art performance.

## Technical Appendix

### Data Pre-Processing

To construct high-quality noun-image pairs from the large-scale CC12M dataset for contrastive learning, we design a two-stage pipeline to extract and filter noun phrases from image captions.

#### Stage 1: Noun Phrase Extraction

We first extract noun phrases from each caption using the spaCy NLP library (Honnibal and Montani 2017). Given a caption  $x$ , we extract syntactic noun chunks  $\mathcal{N}(x) = \{n_1, n_2, \dots, n_k\}$  and retain those that contain at least one noun token (with pos\_ tag NOUN) to ensure semantic relevance. This step eliminates phrases dominated by modifiers or non-content words.

The result is a mapping from each image to a set of candidate noun phrases:

$$\text{Image}_i \rightarrow ['\text{dog}', '\text{park}', '\text{south}', \dots]$$

The extraction process is summarized in Algorithm 1.

#### Stage 2: Generic Phrase Filtering

To enhance the grounding quality of the extracted noun phrases, we further filter out overly generic or non-referential terms such as “reflection”, “southwest” or “background” that lack clear visual correspondence. This is achieved by performing partial string matching against a manually defined exclusion list  $\mathcal{E}$ . A phrase  $p$  is retained only if it contains no substring from  $\mathcal{E}$ :

$$\forall e \in \mathcal{E}, \quad e \notin p$$

The full filtering procedure is outlined in Algorithm 2.

The final output is a cleaned set of noun-image pairs that serve as anchors for downstream contrastive training.

---

**Algorithm 2: Generic Phrase Filtering**

---

**Input:** List of noun phrases, exclusion list  $\mathcal{E}$   
**Output:** Filtered noun phrase list

```
1: for each noun phrase  $p$  in the list do
2:   if  $\forall e \in \mathcal{E}, \quad e \notin p$  then
3:     Keep  $p$ 
4:   else
5:     Discard  $p$ 
6:   end if
7: end for
8: return filtered noun phrases
```

---

## Experimental Setup

### Experimental Environment

In order to satisfy the requirements of the reproducibility checklist, we report our experimental setup in detail here. All experiments in this paper were conducted on a dedicated server equipped with 8×NVIDIA RTX 4090 GPUs (24GB each) and a single Intel Xeon Platinum 8358P CPU. The operating system is Ubuntu Linux 24.04. The compiler and linker environments are configured with GCC 13.2.0 and Binutils 2.42.

The Python environment is based on Python 3.9.20. Major software libraries and dependencies include:

- PyTorch 1.12.1 + CUDA 11.6
- TorchVision 0.13.1 + CUDA 11.6
- MMCV 2.0.0rc3
- MMSegmentation 1.0.0rc4
- SpaCy 3.8.0

To ensure reproducibility, we fix the random seed to 42 in all experiments. And each experiment (including training and evaluation) was run independently on a single RTX 4090 GPU, as our model and training recipes are sufficiently lightweight. All reported results are averaged over three independent runs.

### Hyperparameter Configuration

The hyperparameter settings for the main reported experiments are as follows:

- Loss weights:  $\lambda_1 = 1, \lambda_2 = 1, \lambda_3 = 10, \lambda_4 = 1$
- Learning rate:  $1 \times 10^{-5}$
- Weight decay:  $1 \times 10^{-4}$
- Batch size: 128
- Number of epochs: 1
- Optimizer: SGD

These values are used consistently unless otherwise specified.

### Dataset Details

We evaluate our method on five widely used open-vocabulary semantic segmentation benchmarks: PASCAL VOC (Everingham et al. 2010), Pascal Context (Mottaghi et al. 2014), Cityscapes (Cordts et al. 2016), COCO Object,



and COCO Stuff (Lin et al. 2014; Caesar, Uijlings, and Ferrari 2018). These datasets collectively cover a diverse range of semantic granularity and scene complexity, which makes them suitable for comprehensive evaluation under open vocabulary conditions.

**PASCAL VOC (VOC).** PASCAL VOC is a classical image-based dataset for classification, object detection and segmentation. We use the latest PASCAL VOC 2012 version, which contains 21 semantic categories with an average of 2.5 labeled instances per image. Following prior work, unlabeled regions are treated as a separate *background* class during evaluation.

**Pascal Context (Context).** Pascal Context expands VOC annotations to include 59 object and stuff categories with denser labeling. On average, each image contains 4.8 annotated categories, offering more complex scene understanding challenges. Only labeled pixels are used for evaluation, and background is not treated as an explicit class.

**Cityscapes (City).** Cityscapes focuses on urban street scenes, containing 19 finely annotated semantic categories. The validation set of Cityscapes features high-resolution images with an average of 12.0 labeled categories per image. As with Context, evaluation is performed only on annotated regions. Its strong domain specificity makes it useful for testing model robustness under structured real-world conditions.

**COCO Object (Object).** COCO is a famous dataset built in 2014 and updated in 2017, which concentrates on *Common Objects in Context*. COCO Object includes 80 object classes from the COCO dataset, annotated with instance-level masks. The evaluation treats unlabeled areas as an extra *background* class. The average number of labeled targets per image is 7.2, making it moderately challenging in both category size and visual diversity.

**COCO Stuff (Stuff).** COCO Stuff extends COCO annotations with 91 stuff and 80 object categories (171 total), densely covering nearly every pixel in an image. The validation set has an average of 8.4 semantic regions per image. Evaluation focuses only on labeled pixels.

**Summary .** These datasets collectively evaluate segmentation performance from different semantic settings with wide recognition. Table 3 summarizes their statistics.

Dataset	#Categories	Labels/Image	Background
PASCAL VOC	21	2.5	Yes
Pascal Context	59	4.8	No
Cityscapes	19	12.0	No
COCO Object	81	7.2	Yes
COCO Stuff	171	8.4	No

Table 3: Summary of dataset statistics and evaluation settings.

## References

- Caesar, H.; Uijlings, J.; and Ferrari, V. 2018. COCO-Stuff: Thing and Stuff Classes in Context. In *2018 IEEE/CVF Conference on Computer Vision and Pattern Recognition*, 1209–1218.
- Cai, K.; Ren, P.; Zhu, Y.; Xu, H.; Liu, J.; Li, C.; Wang, G.; and Liang, X. 2023. MixReorg: Cross-Modal Mixed Patch Reorganization is a Good Mask Learner for Open-World Semantic Segmentation. In *2023 IEEE/CVF International Conference on Computer Vision (ICCV)*, 1196–1205.
- Cakir, S.; Gauß, M.; Häppeler, K.; Ounajjar, Y.; Heinle, F.; and Marchthaler, R. 2022. Semantic Segmentation for Autonomous Driving: Model Evaluation, Dataset Generation, Perspective Comparison, and Real-Time Capability. arXiv:2207.12939.
- Cha, J.; Mun, J.; and Roh, B. 2023. Learning to Generate Text-grounded Mask for Open-world Semantic Segmentation from Only Image-Text Pairs. In *Proceedings of the IEEE/CVF Conference on Computer Vision and Pattern Recognition (CVPR)*.
- Changpinyo, S.; Sharma, P.; Ding, N.; and Soricut, R. 2021. Conceptual 12M: Pushing Web-Scale Image-Text Pre-Training To Recognize Long-Tail Visual Concepts. arXiv:2102.08981.
- Chen, J.; Zhu, D.; Qian, G.; Ghanem, B.; Yan, Z.; Zhu, C.; Xiao, F.; Culatana, S. C.; and Elhoseiny, M. 2023. Exploring Open-Vocabulary Semantic Segmentation from CLIP Vision Encoder Distillation Only. In *2023 IEEE/CVF International Conference on Computer Vision (ICCV)*, 699–710.
- Cho, S.; Shin, H.; Hong, S.; Arnab, A.; Seo, P. H.; and Kim, S. 2024. CAT-Seg: Cost Aggregation for Open-Vocabulary Semantic Segmentation. In *Proceedings of the IEEE/CVF Conference on Computer Vision and Pattern Recognition (CVPR)*, 4113–4123.
- Cordts, M.; Omran, M.; Ramos, S.; Rehfeld, T.; Enzweiler, M.; Benenson, R.; Franke, U.; Roth, S.; and Schiele, B. 2016. The Cityscapes Dataset for Semantic Urban Scene Understanding. In *Proc. of the IEEE Conference on Computer Vision and Pattern Recognition (CVPR)*.
- Deng, S.; Zhuo, W.; Xie, J.; and Shen, L. 2023. QA-CLIMS: Question-Answer Cross Language Image Matching for Weakly Supervised Semantic Segmentation. In *Proceedings of the 31st ACM International Conference on Multimedia*, 5572–5583.
- Desai, K.; Kaul, G.; Aysola, Z.; and Johnson, J. 2021. RedCaps: Web-curated image-text data created by the people, for the people. In *NeurIPS Datasets and Benchmarks*.
- Ding, Z.; Wang, J.; and Tu, Z. 2023. Open-vocabulary universal image segmentation with MaskCLIP. In *Proceedings of the 40th International Conference on Machine Learning, ICML’23*. JMLR.org.
- Everingham, M.; Gool, L.; Williams, C. K.; Winn, J.; and Zisserman, A. 2010. The Pascal Visual Object Classes (VOC) Challenge. *Int. J. Comput. Vision*, 88(2): 303–338.
- Ghiasi, G.; Gu, X.; Cui, Y.; and Lin, T.-Y. 2022. Scaling Open-Vocabulary Image Segmentation with Image-Level

- Labels. In *Computer Vision – ECCV 2022: 17th European Conference, Tel Aviv, Israel, October 23–27, 2022, Proceedings, Part XXXVI*, 540–557. Berlin, Heidelberg: Springer-Verlag. ISBN 978-3-031-20058-8.
- Guo, R.; Qu, L.; Niu, D.; Qi, Y.; Yue, W.; Shi, J.; Xing, B.; and Ying, X. 2024. Open-Vocabulary Audio-Visual Semantic Segmentation. In *Proceedings of the 32nd ACM International Conference on Multimedia*, MM ’24, 7533–7541. New York, NY, USA: Association for Computing Machinery. ISBN 9798400706868.
- Honnibal, M.; and Montani, I. 2017. spaCy 2: Natural language understanding with Bloom embeddings, convolutional neural networks and incremental parsing. To appear.
- Jaus, A.; Seibold, C. M.; Reiß, S.; Marinov, Z.; Li, K.; Ye, Z.; Krieg, S.; Kleesiek, J.; and Stiefelhagen, R. 2025. Every Component Counts: Rethinking the Measure of Success for Medical Semantic Segmentation in Multi-Instance Segmentation Tasks. *Proceedings of the AAAI Conference on Artificial Intelligence*, 39(4): 3904–3912.
- Jose, C.; Moutakanni, T.; Kang, D.; Baldassarre, F.; Darcet, T.; Xu, H.; Li, D.; Szafraniec, M.; Ramamonjisoa, M.; Oquab, M.; Siméoni, O.; Vo, H. V.; Labatut, P.; and Bojanowski, P. 2024. DINOv2 Meets Text: A Unified Framework for Image- and Pixel-Level Vision-Language Alignment.
- Kar, M. K.; Nath, M. K.; and Neog, D. R. 2021. A Review on Progress in Semantic Image Segmentation and Its Application to Medical Images. *SN Computer Science*, 2(5): 397.
- Kim, D.; Lin, T.-Y.; Angelova, A.; Kweon, I. S.; and Kuo, W. 2022. Learning Open-World Object Proposals Without Learning to Classify. *IEEE Robotics and Automation Letters*, 7(2): 5453–5460.
- Lai, Z. 2024. Exploring Simple Open-Vocabulary Semantic Segmentation. arXiv:2401.12217.
- Lan, M.; Chen, C.; Ke, Y.; Wang, X.; Feng, L.; and Zhang, W. 2024. ProxyCLIP: Proxy Attention Improves CLIP for Open-Vocabulary Segmentation. In *Computer Vision – ECCV 2024: 18th European Conference, Milan, Italy, September 29–October 4, 2024, Proceedings, Part LXVIII*, 70–88. Berlin, Heidelberg: Springer-Verlag. ISBN 978-3-031-73112-9.
- Li, J.; Li, D.; Xiong, C.; and Hoi, S. 2022. BLIP: Bootstrapping Language-Image Pre-training for Unified Vision-Language Understanding and Generation. In Chaudhuri, K.; Jegelka, S.; Song, L.; Szepesvari, C.; Niu, G.; and Sabato, S., eds., *Proceedings of the 39th International Conference on Machine Learning*, volume 162 of *Proceedings of Machine Learning Research*, 12888–12900. PMLR.
- Li, J.; Selvaraju, R.; Gotmare, A.; Joty, S.; Xiong, C.; and Hoi, S. C. H. 2021. Align before Fuse: Vision and Language Representation Learning with Momentum Distillation. In Ranzato, M.; Beygelzimer, A.; Dauphin, Y.; Liang, P.; and Vaughan, J. W., eds., *Advances in Neural Information Processing Systems*, volume 34, 9694–9705. Curran Associates, Inc.
- Lin, T.-Y.; Maire, M.; Belongie, S.; Hays, J.; Perona, P.; Ramanan, D.; Dollár, P.; and Zitnick, C. L. 2014. Microsoft COCO: Common Objects in Context. In Fleet, D.; Pajdla, T.; Schiele, B.; and Tuytelaars, T., eds., *Computer Vision – ECCV 2014*, 740–755. Cham: Springer International Publishing. ISBN 978-3-319-10602-1.
- Liu, Q.; Wen, Y.; Han, J.; Xu, C.; Xu, H.; and Liang, X. 2022. Open-World Semantic Segmentation via Contrast-ing and Clustering Vision-Language Embedding. In *Computer Vision – ECCV 2022: 17th European Conference, Tel Aviv, Israel, October 23–27, 2022, Proceedings, Part XX*, 275–292. Berlin, Heidelberg: Springer-Verlag. ISBN 978-3-031-20043-4.
- Liu, Y.; Ge, P.; Wang, G.; Liu, Q.; and Huang, D. 2025. Multi-Grained Contrastive Learning for Text-Supervised Open-Vocabulary Semantic Segmentation. *ACM Trans. Multimedia Comput. Commun. Appl.*, 21(3).
- Lüddecke, T.; and Ecker, A. 2022. Image Segmentation Using Text and Image Prompts. In *Proceedings of the IEEE/CVF Conference on Computer Vision and Pattern Recognition (CVPR)*, 7086–7096.
- Luo, H.; Bao, J.; Wu, Y.; He, X.; and Li, T. 2023. Seg-CLIP: patch aggregation with learnable centers for open-vocabulary semantic segmentation. In *Proceedings of the 40th International Conference on Machine Learning*, ICML’23. JMLR.org.
- Mottaghi, R.; Chen, X.; Liu, X.; Cho, N.-G.; Lee, S.-W.; Fidler, S.; Urtasun, R.; and Yuille, A. 2014. The Role of Context for Object Detection and Semantic Segmentation in the Wild. In *2014 IEEE Conference on Computer Vision and Pattern Recognition*, 891–898.
- Mukhoti, J.; Lin, T.-Y.; Poursaeed, O.; Wang, R.; Shah, A.; Torr, P. H.; and Lim, S.-N. 2023. Open Vocabulary Semantic Segmentation With Patch Aligned Contrastive Learning. In *Proceedings of the IEEE/CVF Conference on Computer Vision and Pattern Recognition (CVPR)*, 19413–19423.
- Perez, E.; Strub, F.; de Vries, H.; Dumoulin, V.; and Courville, A. 2018. FiLM: visual reasoning with a general conditioning layer. In *Proceedings of the Thirty-Second AAAI Conference on Artificial Intelligence and Thirtieth Innovative Applications of Artificial Intelligence Conference and Eighth AAAI Symposium on Educational Advances in Artificial Intelligence*, AAAI’18/IAAI’18/EAAI’18. AAAI Press. ISBN 978-1-57735-800-8.
- Radford, A.; Kim, J. W.; Hallacy, C.; Ramesh, A.; Goh, G.; Agarwal, S.; Sastry, G.; Askell, A.; Mishkin, P.; Clark, J.; Krueger, G.; and Sutskever, I. 2021. Learning Transferable Visual Models From Natural Language Supervision. In Meila, M.; and Zhang, T., eds., *Proceedings of the 38th International Conference on Machine Learning*, volume 139 of *Proceedings of Machine Learning Research*, 8748–8763. PMLR.
- Rao, Y.; Zhao, W.; Chen, G.; Tang, Y.; Zhu, Z.; Huang, G.; Zhou, J.; and Lu, J. 2022. DenseCLIP: Language-Guided Dense Prediction with Context-Aware Prompting. In *Proceedings of the IEEE Conference on Computer Vision and Pattern Recognition (CVPR)*.
- Ren, P.; Li, C.; Xu, H.; Zhu, Y.; Wang, G.; Liu, J.; Chang, X.; and Liang, X. 2023. ViewCo: Discovering Text-Supervised

- Segmentation Masks via Multi-View Semantic Consistency. In *The Eleventh International Conference on Learning Representations*.
- Sharma, P.; Ding, N.; Goodman, S.; and Soricut, R. 2018. Conceptual Captions: A Cleaned, Hypernymed, Image Alt-text Dataset For Automatic Image Captioning. In Gurevych, I.; and Miyao, Y., eds., *Proceedings of the 56th Annual Meeting of the Association for Computational Linguistics (Volume 1: Long Papers)*, 2556–2565. Melbourne, Australia: Association for Computational Linguistics.
- Sun, W.; Du, Y.; Liu, G.; Kompella, R.; and Snoek, C. G. M. 2024. Training-Free Semantic Segmentation via LLM-Supervision. *CoRR*, abs/2404.00701.
- Tang, S.; Luo, Z.; Wang, Y.; Wang, L.; Lu, H.; Su, W.; and Liu, L. 2024. LOVD: Large-and-Open Vocabulary Object Detection. In *Proceedings of the 32nd ACM International Conference on Multimedia, MM '24*, 9321–9329. New York, NY, USA: Association for Computing Machinery. ISBN 9798400706868.
- Thomee, B.; Shamma, D. A.; Friedland, G.; Elizalde, B.; Ni, K.; Poland, D.; Borth, D.; and Li, L.-J. 2016. YFCC100M: the new data in multimedia research. *Commun. ACM*, 59(2): 64–73.
- Wang, H.; Vasu, P. K. A.; Faghri, F.; Vemulapalli, R.; Farajtabar, M.; Mehta, S.; Rastegari, M.; Tuzel, O.; and Pouransari, H. 2024a. SAM-CLIP: Merging Vision Foundation Models Towards Semantic and Spatial Understanding. In *Proceedings of the IEEE/CVF Conference on Computer Vision and Pattern Recognition (CVPR) Workshops*, 3635–3647.
- Wang, L.; Li, D.; Liu, H.; Peng, J.; Tian, L.; and Shan, Y. 2022a. Cross-Dataset Collaborative Learning for Semantic Segmentation in Autonomous Driving. *Proceedings of the AAAI Conference on Artificial Intelligence*, 36(3): 2487–2494.
- Wang, Z.; Yu, J.; Yu, A. W.; Dai, Z.; Tsvetkov, Y.; and Cao, Y. 2022b. SimVLM: Simple Visual Language Model Pre-training with Weak Supervision. In *International Conference on Learning Representations*.
- Wang, Z.; Zhou, W.; Xu, J.; and Peng, Y. 2024b. SIA-OVD: Shape-Invariant Adapter for Bridging the Image-Region Gap in Open-Vocabulary Detection. In *Proceedings of the 32nd ACM International Conference on Multimedia, MM '24*, 4986–4994. New York, NY, USA: Association for Computing Machinery. ISBN 9798400706868.
- Wu, J.-J.; Chang, A. C.-H.; Chuang, C.-Y.; Chen, C.-P.; Liu, Y.-L.; Chen, M.-H.; Hu, H.-N.; Chuang, Y.-Y.; and Lin, Y.-Y. 2024. Image-Text Co-Decomposition for Text-Supervised Semantic Segmentation. In *Proceedings of the IEEE/CVF Conference on Computer Vision and Pattern Recognition (CVPR)*, 26794–26803.
- Xie, J.; Xiang, J.; Chen, J.; Hou, X.; Zhao, X.; and Shen, L. 2022. C2AM: Contrastive Learning of Class-Agnostic Activation Map for Weakly Supervised Object Localization and Semantic Segmentation. In *Proceedings of the IEEE/CVF Conference on Computer Vision and Pattern Recognition (CVPR)*, 989–998.
- Xing, Y.; Kang, J.; Xiao, A.; Nie, J.; Ling, S.; and Lu, S. 2023. Rewrite Caption Semantics: Bridging Semantic Gaps for Language-Supervised Semantic Segmentation. In *Advances in Neural Information Processing Systems*.
- Xu, J.; De Mello, S.; Liu, S.; Byeon, W.; Breuel, T.; Kautz, J.; and Wang, X. 2022. GroupViT: Semantic Segmentation Emerges From Text Supervision. In *Proceedings of the IEEE/CVF Conference on Computer Vision and Pattern Recognition (CVPR)*, 18134–18144.
- Xu, J.; Hou, J.; Zhang, Y.; Feng, R.; Wang, Y.; Qiao, Y.; and Xie, W. 2023. Learning open-vocabulary semantic segmentation models from natural language supervision. In *Proceedings of the IEEE/CVF Conference on Computer Vision and Pattern Recognition*, 2935–2944.
- Yi, M.; Cui, Q.; Wu, H.; Yang, C.; Yoshie, O.; and Lu, H. 2023. A Simple Framework for Text-Supervised Semantic Segmentation. In *Proceedings of the IEEE/CVF Conference on Computer Vision and Pattern Recognition (CVPR)*, 7071–7080.
- Zhang, P.; Li, X.; Hu, X.; Yang, J.; Zhang, L.; Wang, L.; Choi, Y.; and Gao, J. 2021. VinVL: Revisiting Visual Representations in Vision-Language Models. In *2021 IEEE/CVF Conference on Computer Vision and Pattern Recognition (CVPR)*, 5575–5584.
- Zhou, B.; Khosla, A.; Lapedriza, A.; Oliva, A.; and Torralba, A. 2016. Learning Deep Features for Discriminative Localization. In *2016 IEEE Conference on Computer Vision and Pattern Recognition (CVPR)*, 2921–2929.
- Çağrı Kaymak; and Uçar, A. 2018. A Brief Survey and an Application of Semantic Image Segmentation for Autonomous Driving. arXiv:1808.08413.